

Persistent Regimes and Extreme Events of the North Atlantic Atmospheric Circulation

BY CHRISTIAN L. E. FRANZKE

British Antarctic Survey, Cambridge, UK

Society is increasingly impacted by natural hazards which cause significant damage in economic and human terms. Many of these natural hazards are weather and climate related. Here we show that North Atlantic atmospheric circulation regimes affect the propensity of extreme wind speeds in Europe. We also show evidence that extreme wind speeds are long-range dependent, follow a Generalised Pareto distribution and are serially clustered. Serial clustering means that storms come in bunches and, hence, do not occur independently. We discuss the use of waiting time distributions for extreme event recurrence estimation in serially dependent time series.

Keywords: Circulation Regimes, Extremes, Long-Range Dependence, Clustering

1. Introduction

An important part of European weather and climate are wind storms. European wind storms can cause economic damage and insurance losses on the order of more than one billion Euro per year and rank as the second highest cause of global natural catastrophe insurance loss (Malmquist 1999). Many of these hazard events are not independent; for instance, severe storms can occur in trains of storms. Examples of such recurring storms include January 2008 (Paula and Resi) and March 2008 (Emma, Johanna and Kirsten) which each caused damages on the order of 1bn Euros (e.g. guycarp.com). Also the 2007 floods in the UK were caused by a succession of weather systems slowly moving across the UK which were likely caused by the jet stream located further south than normal (Blackburn et al. 2008). Another typical climate phenomenon in the North Atlantic region are nearly stationary blocking anticyclones which can cause heat waves, extreme cold spells (Cattiaux et al. 2010) and drought conditions.

The Intergovernmental Panel on Climate Change (IPCC 2012) has stated that it is likely that anthropogenic climate change leads to changes in the frequency and intensity of weather and climatic extreme events (Trenberth et al. 2007, Rahmstorf and Coumou 2011). The first six months of 2011 incurred insurance losses of about US\$60bn which is about five times the average for the first six months of the year in the period 2001-2010 (Press release by MunichRe 2011). However, it is not clear how much of this loss increase is due to increasing populations in vulnerable regions, a significant increase in natural extreme events or random fluctuations in the rate of natural hazards. This illustrates the challenge society is facing in mitigating the effects of natural hazards.

40 It has long been recognised that low-frequency large-scale circulation patterns
41 have a significant impact on surface weather and climate. These circulation patterns
42 or regimes have been shown to affect extreme temperatures, cyclones, wind speeds
43 and precipitation (Thompson and Wallace 2001, Yiou and Nogaj 2004, Raible 2007,
44 Yiou et al. 2008, Yin and Branstator 2008). Since the regimes also affect cloud
45 cover and the distribution of aerosols they may also influence the climate response
46 to increasing greenhouse gas emissions and climate sensitivity. Since low-frequency
47 waves are well represented in climate models this offers the potential to statistically
48 extract information about extreme events (which might not be well represented
49 in climate models) from simulations like the frequency of occurrence of extreme
50 events. This might enable projections of how extreme events change in seasonal
51 and decadal scale predictions and future climate projections. Many businesses and
52 decision-makers need this kind of information.

53 Traditional extreme value statistics are based on the premise that extreme events
54 occur independently from each other. However, this is rarely the case for weather
55 and climatic extremes where these extreme events tend to serially cluster as dis-
56 cussed above. In the traditional framework no account is taken of the temporal
57 dependency structure of weather and climate variables that are present in many
58 natural time series. The temporal dependence can lead to the clustering of extremes
59 and traditional extreme value statistics has to be adjusted to take account of this
60 (Berman 1964, Leadbetter and Rootzen 1988, Bunde et al. 2005, Garrett and Müller
61 2008). This temporal dependence impedes our ability to estimate return periods,
62 which now also requires the prediction of the clusters of extreme events, which are
63 important for many practical applications.

64 The purpose of this contribution is to discuss the dependence structure and the
65 empirical extreme value distribution of surface wind speeds and the occurrence of
66 clustered wind speed extremes. We will also discuss how the regimes of the eddy-
67 driven Atlantic jet stream (Franzke et al. 2011) affect the propensity of extreme
68 events and the temporal dependence of wind speeds. We also provide evidence that
69 surface wind speeds follow a Generalised Pareto extreme value distribution and that
70 their amplitude is bounded; consistent with theoretical predictions. We will discuss
71 the use of waiting time distributions as an alternative to return times inferred
72 from extreme value statistics. Waiting time distributions are a natural measure for
73 extremes of dependent data.

74 In section 2 we will describe the data, including the Jet Latitude Index (JLI)
75 which is used as a proxy of North Atlantic climate variability (Woollings et al.
76 2010, Franzke and Woollings 2011, Franzke et al. 2011). Section 3 examines the
77 persistence properties and extreme value characteristics of North Atlantic surface
78 wind speeds while section 4 presents how persistent circulation regimes affect the
79 propensity of extreme events. Here we focus on extreme wind speeds, deviations
80 from Gaussianity in 500 hPa geopotential height as a first measure of extremes, and
81 clustering of extremes. Previous studies mainly focused on the relationship between
82 circulation regimes and temperature and precipitation extremes. A summary and
83 discussion are given in section 5.

2. Data

84

85 Data are used from the European Centre for Medium-Range Weather Forecasts
 86 (ECMWF) ERA-40 Re-Analysis (Uppala et al. 2005). We use daily mean fields for
 87 zonal u and meridional v wind fields and 500 hPa geopotential height. The wind
 88 speed is computed as $\sqrt{u^2 + v^2}$.

89 As a North Atlantic climate variability proxy we use the jet latitude index
 90 (JLI) which is a measure of North Atlantic climate variability and in particular
 91 of the position of the lower tropospheric eddy-driven jet stream (Woollings et al.
 92 2010, Franzke and Woollings 2011). This index covers the period 1 December 1958
 93 through 28 February 2001. The JLI is derived in the following way: (1) A mass-
 94 weighted average of the daily mean zonal wind is taken over the vertical levels 925,
 95 850, 775 and 700 hPa and over the Atlantic sector $0^\circ - 60^\circ\text{W}$. (2) Winds poleward
 96 of 75°N and equatorwards of 15°N are neglected. (3) The resulting wind field is low-
 97 pass filtered, only retaining periods greater than 10 days. (4) The JLI is defined as
 98 the latitude at which the maximum wind speed is found. (5) A smooth annual cycle
 99 is subtracted from the resulting time series. See Woollings et al. (2010) for more
 100 details, where it is also shown that this index describes jet stream variations which
 101 are associated with both the North Atlantic Oscillation (NAO) and the East At-
 102 lantic (EA) teleconnection pattern and, therefore, represents a good general proxy
 103 of North Atlantic climate variability. Based on the JLI we will compute composite
 104 fields of various quantities like skewness, kurtosis and extreme wind speeds. The
 105 composites of the wind speed data are computed from unfiltered data.

106

3. Persistence and Extreme Events

107

(a) Persistence of the Atmospheric Circulation

108 Persistence is one of the most fascinating and important characteristics of the
 109 atmosphere. By persistence we mean the atmosphere's tendency to maintain its cur-
 110 rent state. One of the simplest weather forecasting models is a persistence forecast
 111 where one predicts that tomorrow will be like today. This persistence forecast has a
 112 surprisingly good forecast skill. Such a forecasting model would be Markovian. The
 113 Markov property implies that the next state only depends on the current state but
 114 not on any past states. However, there is growing evidence that many climate vari-
 115 ables have a more complicated temporal dependence structure (Koscielny-Bunde et
 116 al. 1998, Vyushin et al. 2009, Franzke 2010, 2012a, Ghil et al. 2011). This temporal
 117 dependence structure also indicates knowledge of the past is needed to forecast the
 118 next state. This temporal dependence of climate variables leads to so-called stochas-
 119 tic trends (Franzke 2010, 2012a) and the serial clustering of extremes (Bunde et al.
 120 2005). Stochastic trends are trends which arise due to persistence and not due to
 121 external forcing like greenhouse gas emissions. Long-range dependent time series
 122 can exhibit stochastic trends over much longer periods of time than say a Marko-
 123 vian process and thus the detection of trends and attribution of drivers becomes
 124 much harder. The disentanglement of stochastic and deterministic trends is a field
 125 of active research (e.g. Barbosa 2011, Franzke 2010, 2012a).

126 A measure of the temporal dependence and persistence of a time series is the
 127 long-range dependency parameter d (Beran 1994). A process is long-range depen-
 128 dent when the prediction of its next state depends on the entirety of its past. An

129 imprint of this dependence structure is that the covariance $r(k) = Cov(X(k), X(0))$
 130 decays slowly, as $k \rightarrow \infty$, so that

$$\sum_{k=0}^{\infty} |r(k)| \rightarrow \infty. \quad (3.1)$$

131 The parameter d can be defined by specifying long-range dependence as a power-
 132 law like decay of the autocorrelation function. Thus, we define that a stationary
 133 process is long-range dependent if it has autocorrelation function r such that

$$r(k) \sim k^{2d-1} \text{ as } k \rightarrow \infty \quad (3.2)$$

134 where $0 < d < \frac{1}{2}$. This power law decay of the autocorrelation function is not
 135 integrable and will lead to a blow up as described by Eq. (3.1).

136 This slow decay of the covariances means that the values of the process X are
 137 strongly dependent over long periods of time. This contrasts with the more familiar
 138 short-range dependent process where $\sum_{k=0}^{\infty} |r(k)| = C < \infty$ and the correlations
 139 typically decay exponentially. In a short-range dependent process the next state only
 140 depends on the current state and the recent past. The archetype of a short-range
 141 dependent process is a first order Markov process where the next state depends
 142 only on the present state. See Beran (1994) for more details.

143 In order to estimate d we used the semi-parametric power spectral method of
 144 Geweke & Porter-Hudak (1983) and Hurvich and Deo (1999). Spectral methods
 145 find d by estimating the spectral slope of the low frequencies. The periodogram is
 146 used, which is an estimate of the spectral density of a finite-length time series and
 147 is given by:

$$\hat{S}(\lambda_j) = \frac{1}{N} \left| \sum_{t=1}^N X(t) e^{-i2\pi t \lambda_j} \right|^2, \quad j = 1, \dots, [N/2], \quad (3.3)$$

148 where $\lambda_j = j/N$ is the frequency and the square brackets denote rounding down.
 149 A series with LRD has a spectral density proportional to $|\lambda|^{-2d}$ close to the origin.
 150 Since $\hat{S}(\lambda)$ is an estimator of the spectral density, d is estimated by a regression
 151 of the logarithm of the periodogram versus the logarithm of the frequency λ . Thus
 152 having calculated the spectral density estimate $\hat{S}(\lambda)$, semi-parametric estimators
 153 fit a power law of the form $f(\lambda, b, d) = b|\lambda|^d$, where b is a scaling factor. The
 154 number of frequencies for the log-periodogram regression is computed with the
 155 plug-in selector derived by Hurvich and Deo (1999). Confidence intervals and bias
 156 correction for this estimator have been derived by Hurvich and Deo (1999) and the
 157 confidence intervals are asymptotically Gaussian distributed. The reliability of this
 158 estimator has been validated by Franzke et al. (2012).

159 The long-range dependence parameter $d = 0$ indicates that no temporal de-
 160 pendence is present in the data; thus the data are white noise. Positive d values
 161 indicate persistence and negative denote anti-persistence. Anti-persistence has a
 162 so-called blue noise power spectrum with the least power at low frequencies and
 163 with monotonically increasing variance towards high-frequencies. Furthermore, in
 164 a pure long-range dependent process for $d \rightarrow 0$ a singularity is approached and the
 165 dependence structure goes directly from long-range dependent to independent. The
 166 reason for this can be illustrated with the power spectrum. When testing for long-
 167 range dependence one is interested in the long-term behaviour of the time series and

168 thus the low-frequencies. At these time scales the short-term dependent behaviour
 169 is negligible and is effectively white noise and independent at long time scales. If
 170 the time series exhibits long-range dependence then there will be a power-law like
 171 slope visible in the power spectrum for the lowest frequencies; otherwise the power
 172 spectrum is flat at low frequencies indicating white noise behaviour.

173 Fig. 1 shows the geographical distribution of d values which are significantly
 174 different from 0 for the North Atlantic region. The figure reveals that surface wind
 175 speeds are significantly long-range dependent. Most d values are positive, only a
 176 small area in the western North Atlantic has negative values. The largest d values
 177 occur over western North Africa, also the UK and Scandinavia have enhanced d
 178 values. We repeated this analysis with linearly detrended wind speed data and get
 179 very similar results (not shown). This suggests that the impact of possible trends
 180 is negligible. This provides evidence that surface wind speeds in the North Atlantic
 181 region are long-range dependent. Below we will put forward the idea that this long-
 182 range dependency might be the imprint of non-stationarities due to the regime
 183 behaviour of the jet stream.

184 (b) *Extremes of the Atmospheric Circulation*

185 In order to examine the extreme value characteristics of surface wind speeds
 186 we use a threshold exceedance approach and fit a Generalised Pareto Distribution
 187 (GPD, Coles 2001) whose PDF is given by

$$f_{(\xi,\mu,\sigma)}(x) = \frac{1}{\sigma} \left(1 + \frac{\xi(x - \mu)}{\sigma} \right)^{(-\frac{1}{\xi}-1)} \quad (3.4)$$

188 where ξ denotes the shape parameter, μ the threshold (or location parameter) and
 189 σ the scale parameter. The shape and scale parameters are fitted with a standard
 190 maximum likelihood approach (Coles 2001). The GPD is generalised in the sense
 191 that it contains three special cases: (i) when $\xi > 0$ the GPD is equivalent to an
 192 ordinary Pareto distribution, (ii) when $\xi = 0$ the GPD becomes an exponential
 193 distribution and (iii) for $\xi < 0$ the GPD is a short-tailed Pareto type II distribution
 194 (Coles 2001). The standard asymptotic properties of the maximum likelihood esti-
 195 mator cannot be proven for shape parameters less than -0.5 and thus the confidence
 196 intervals cannot be reliably computed but this does not necessarily mean that the
 197 parameter estimates are not robust.

198 We estimate the GPD parameters from unfiltered wind speed data. Fig. 2 shows
 199 the shape and scale parameters of a GPD distribution. As a threshold we selected
 200 the 90th percentile value of the wind speed at each grid point. The parameter es-
 201 timates are relatively stable for a range of different thresholds (see Fig. 2) and a
 202 visual inspection of quantile-quantile plots at some locations shows that the wind
 203 speed data follow a GPD (not shown). This provides confidence that surface wind
 204 speed extremes indeed can be described by a GPD. Furthermore, the shape param-
 205 eter is negative. This indicates that extreme surface wind speeds are bounded. The
 206 shape parameter reaches its maximum over the central North Atlantic but also the
 207 UK, Scandinavia and Central Europe exhibit a large scale parameter. Our results
 208 are consistent with the study by Fawcett and Walshaw (2006) which also find that
 209 extreme wind speeds follow a GPD with mostly negative shape parameters.

210 That the unfiltered wind speed extremes are bounded is consistent with the
 211 theoretical findings of Majda et al. (2009). They show that while the normal form
 212 of stochastic climate models allows for a power-law like decay of the PDF tail over
 213 some range of values, the ultimate decay will be squared exponential (i.e. Gaus-
 214 sian; see their equation 11); thus very large values have a vanishing probability.
 215 This is in contrast to the results of Sardeshmukh and Sura (2009) and Sura (2011).
 216 They consider only a linear model with state-dependent noise and neglect the non-
 217 linearity. Majda et al. (2009) and Franzke (2012b) have shown that the nonlinear
 218 interaction between slow and fast modes is producing the state-dependent noise in
 219 the normal form of stochastic climate models and is causing the tail of the PDF
 220 to decay according to a squared exponential function. This suggests that nonlinear
 221 interactions cannot be neglected and are a possible cause of the deviations from
 222 Gaussianity.

223 (c) Clustering of Atmospheric Circulation Extremes

224 While long-range dependence and extreme value statistics seem at first sight
 225 fairly unrelated to each other, in fact the opposite is the case. Long-range depen-
 226 dence has a rather strong impact on extreme value statistics, especially the return
 227 periods of extreme values. Long-range dependence leads to the clustering of ex-
 228 tremes. Clustering of extremes means that there exist time periods where values
 229 are more likely to exceed the extreme value threshold than if they were to occur
 230 independent from each other. Likewise, there also exist periods where less extremes
 231 occur than one would expect if they were to occur independently. This means that
 232 extreme events are likely followed by other extreme events and that there are long
 233 periods when no extreme events occur. A prime example is the serial clustering of
 234 storms (Mailier et al. 2006) as alluded to in the introduction.

235 Traditional extreme value theory assumes that the data under consideration are
 236 independent and identically distributed (iid). For many climate time series this is
 237 not the case because these time series are autocorrelated and extreme value theory
 238 has been extended for dependent time series (Coles 2001, Beirlant et al. 2004).
 239 Extreme value theory can be extended to the case of short-range dependent time
 240 series by introducing the extremal index which adjusts the parameters of the GPD
 241 (Coles 2001). The extremal index is a measure of the clustering of extremes which
 242 adjusts extreme value distributions for serially short-range dependent time series
 243 (Coles 2001). In the presence of long-range dependence the GPD can still describe
 244 the amplitude distribution and we have provided empirical evidence for this in
 245 the previous section; see also Franzke (2012c). However, the presence of long-range
 246 dependence and thus clustering might affect the return period estimates based on
 247 the GPD in ways which one cannot account for solely with the extremal index and
 248 is an active area of research.

249 The extremal index θ is computed by using the method of Hamidieh et al.
 250 (2009). It characterises the extent of temporal dependency of extreme events and is
 251 inversely proportional to the average cluster size. The approach by Hamidieh et al.
 252 (2009) is based on the asymptotic scaling properties of block-maxima and resam-
 253 pling. The maxima of blocks of size m scale as $m^{\frac{1}{\alpha}}$, where α is the tail exponent.
 254 Thus, by examining a sequence of dyadic block sizes $m(j) = 2^j$ and resampling one
 255 can estimate the extremal index $\theta(j)$ and the corresponding uncertainty bounds

(see Hamidieh et al. (2009) for more details). Evidence for clustering of extremes is given if θ turns out to be stable over a range of scales. An extremal index value close to 1 indicates almost independent extremes. In order to find θ values which are robust over a range of scales we use the non-parametric Kruskal-Wallis test (Hamidieh et al. 2009). We use this test to assess whether the medians over a scale range are statistically indistinguishable at a level of 5%. Furthermore, the resampling approach provides error intervals which provide a means to test whether the extremal index values are statistically significant different from 1. We also performed a field significance test (Livezey and Chen 1983) and found the results to be significant at the 5% level.

Fig. 3 shows the extremal index of surface wind speeds (only significant values at the 5% level are displayed). While the distribution of the extremal index is noisy the figure nonetheless provides evidence that extreme surface wind speeds are clustered in the North Atlantic region. Especially the UK, the Iberian peninsula, Germany and France as well as south-west Greenland, Latin America and Africa show extremal index values significantly different from 1 which indicate a propensity to clustering of wind speed events.

The fact that extreme wind speeds are clustered is consistent with the long-range dependence of wind speeds. In the next section we will provide evidence for regime behaviour which is one possible mechanism for the observed long-range dependence and clustering of extremes.

4. Persistent North Atlantic Regimes and Extremes

One of the most fascinating aspects of climate variability is that it can be described by just a few teleconnection patterns. This ability is attractive because this would not only allow for a very efficient description of the atmosphere but also offer the prospect of skillful long-range predictions. The quest to decompose the low-frequency atmospheric circulation into just a few recurring or preferred circulation patterns is long ongoing. The earliest attempts have been made by Defand (1924) and Walker and Bliss (1932). These studies identified the North Atlantic Oscillation (NAO) as the dominant teleconnection pattern in the North Atlantic region which exerts a significant influence on surface weather and climate. Other well known teleconnection patterns in the North Atlantic region are the East Atlantic (EA) and the Scandinavian patterns. These patterns are typically identified by Empirical Orthogonal Function (EOF) analysis (Barnston and Livezey 1987), Gaussian mixture analysis (Smyth et al. 1999), deviations from Gaussianity (Kimoto and Ghil 1993) or cluster analysis (Cheng and Wallace 1993, Cassou 2008).

In order to examine the relationship between persistent circulation regimes and extreme events here we are using the circulation regimes identified by Franzke et al. (2011). They used a Hidden Markov Model (HMM) to identify persistent regime states. A HMM identifies preferred persistent states in phase space by simultaneously estimating a Gaussian mixture model and a Markov transition matrix. The Markov transition matrix describes the temporal evolution of the regimes (Majda et al. 2006, Franzke et al. 2008, 2009, 2011). As a proxy of North Atlantic climate variability the JLI has been used and three significant persistent regime states have been identified which correspond to a Northern, Southern and Central jet state (see Fig. 2 of Franzke et al. (2011)). Franzke et al. (2011) show that the regimes well

302 describe the storm tracks and that Rossby wave breaking plays a large role in the
 303 maintenance of the regimes.

304 The regime behaviour and long-range dependence are likely closely related.
 305 Regime behaviour is a case of non-stationarity which is able to induce long-range
 306 dependence (Klemes 1974). One of the simplest explanations of long-range depen-
 307 dence is that a system persists for long periods of time above or below its climato-
 308 logical mean value. This is exactly what happens for the jet stream regimes; they
 309 fluctuate for long periods of time around either their northern, southern or central
 310 states (Franzke et al. 2011). This suggests that the jet stream regime behaviour is
 311 a likely cause of the observed long-range dependence.

312 As we will show next these circulation regimes determine the propensity of
 313 extremes. One sign of the possible presence of extremes are deviations from Gaus-
 314 sianity. For instance, deviations from Gaussianity can indicate that large values
 315 occur more frequently than one would expect if they were from the Gaussian dis-
 316 tribution. Nakamura and Wallace (1991) and Holzer (1996) provided evidence that
 317 deviations from Gaussianity in geopotential height fields are associated with ex-
 318 treme events. The first measures of deviations from Gaussianity are the skewness
 319 and kurtosis. Skewness indicates the degree of symmetry around the mean value;
 320 a Gaussian distribution has a skewness of zero. Kurtosis denotes the peakedness of
 321 the distribution; i.e. if it has more or less mass in the tail of its distribution than a
 322 Gaussian distribution. The skewness is defined as

$$s = \frac{\frac{1}{n} \sum_{i=1}^n (x_i - \bar{x})^3}{\left(\frac{1}{n} \sum_{i=1}^n (x_i - \bar{x})^2\right)^{\frac{3}{2}}} \quad (4.1)$$

323 and the excess kurtosis as

$$k = \frac{\frac{1}{n} \sum_{i=1}^n (x_i - \bar{x})^4}{\left(\frac{1}{n} \sum_{i=1}^n (x_i - \bar{x})^2\right)^2} - 3 \quad (4.2)$$

324 where n denotes the length of the time series x_i , and \bar{x} the mean value of the time
 325 series.

326 In Fig. 4 is displayed the skewness and in Fig. 5 the excess kurtosis of 500
 327 hPa geopotential height. These figures show that the jet stream regimes have an
 328 impact on the deviations of Gaussianity in the upper tropospheric circulation in
 329 the North Atlantic region and over Europe. The Southern jet regime is associated
 330 with negative skewness and positive excess kurtosis on the equatorward flank of
 331 the jet stream and negative skewness and positive kurtosis over south-east Europe.
 332 The Northern regime is associated with positive skewness on the equatorward flank
 333 of the jet stream and negative skewness over central Europe and negative kurtosis
 334 over the Norwegian and Barents sea, while the Central jet regime is associated with
 335 positive skewness on the equatorward flank of the jet stream, positive skewness over
 336 central Europe and negative skewness west of the Iberian peninsula and negative
 337 kurtosis on the poleward flank of the jet stream.

338 These changes are likely due to changes in preferred locations of blocking in
 339 the jet regimes (Franzke et al. 2011). The northern jet regime is associated with
 340 blocking anti-cyclones mainly over southwestern Europe, the southern jet regime
 341 with Greenland blockings and the central jet regime with a reduction of blocking
 342 systems (Franzke et al. 2011). These changes in blocking and corresponding changes

343 in deviations of Gaussianity are consistent with the findings of White (1980) and
344 Rennert and Wallace (2009). On the other hand, Luxford and Woollings (2012)
345 put forward the idea that the observed deviations from Gaussianity are just a
346 consequence of the jet stream shifts and do not necessarily imply nonlinear dynamics
347 and changes in blocking locations.

348 Next we examine how the regimes affect the occurrence of extreme wind speeds.
349 For this purpose we computed the 99.9th percentile of unfiltered wind speeds. Fig.
350 6 reveals that the regime states also affect extreme wind speeds over the North
351 Atlantic and the UK. During the Southern jet state extreme wind speeds are more
352 likely to occur on the poleward side of the jet while during the Northern jet state
353 they are more likely to occur on the equatorward side. During the Central jet state
354 extreme wind speeds are likely to occur in a small band north-west of Ireland. The
355 extreme wind speed results are robust against a change in the exact percentile level;
356 choosing the 99th percentile level gives broadly the same results (not shown).

357 The statistical significance of the skewness, kurtosis and extreme wind speeds
358 are tested by using a bootstrap approach. This tests whether the composite fields
359 could have arisen from sampling issues. Our results suggest that the skewness, kur-
360 tosis and extreme wind speeds are unlikely to be the result of sampling variability.
361 We also performed a field significance test (Livezey and Chen 1983) and found
362 the results to be significant at the 5% level. These results reveal that circulation
363 regimes of the North Atlantic jet stream have a statistically significant impact on
364 the propensity of extreme events.

365 5. Summary and Discussion

366 In this contribution we have provided evidence that circulation regimes of the North
367 Atlantic eddy-driven jet stream affect the propensity of extremes. In the case that
368 seasonal-to-interannual prediction systems can skillfully predict the regime states
369 of the jet stream or their changes in frequency of occurrence this would offer the
370 prospect of probabilistic forecasts of the likely number of extreme events for the
371 next season or year. This kind of information is needed by many businesses and
372 decision-makers. It has to be noted that many climate models still have problems
373 simulating blockings, which are strongly related to the jet stream regimes. This
374 is likely related to the nonlinear wave breaking which is essential in the life cycle
375 of blockings. Capturing the wave breaking features likely requires high horizontal
376 resolutions.

377 We also provided evidence of long-range dependence of surface wind speeds. The
378 occurrence of circulation regimes are a possible explanation of this property because
379 they introduce non-stationary behaviour. It is well known that non-stationarity
380 can cause long-range dependent behaviour. The fact that the wind speed extremes
381 are serially clustered is consistent with both the long-range dependence and the
382 regime behaviour (i.e. the non-stationarity). For instance, in Fig. 7 is displayed the
383 wind speed time series at a grid point close to London. The time series looks non-
384 stationary with periods with persistent high or low wind speeds. These persistent
385 periods of high and low wind speeds are likely related to the regime behaviour of
386 the jet stream and the long-range dependence.

387 This finding also has wider implications for climate change because long-range
388 dependent processes can produce apparent trends over rather long periods of time

389 (Franzke 2010, 2012a) and there is evidence that surface temperatures are long-
390 range dependent (Koscielny-Bunde et al. 1998). Also non-stationarities or regime
391 behaviour can cause apparent trends. A typical HMM realisation, which is a paradigmatic
392 non-stationary process, as displayed in Franzke et al. (2008) shows how regime
393 behaviour can cause an apparent trend (see their Fig. 1b). However, there will be no
394 trend for sufficiently long HMM realisations. The likely connection between climatic
395 regime behaviour and climate trends needs further research.

396 Furthermore, the fact that extreme wind speeds cluster suggests that return
397 periods are not necessarily a useful measure. This is even more complicated by the
398 presence of long-range dependence which will link even far apart extreme events.
399 This linking will negate traditional attempts to de-cluster the time series (Coles
400 2001). This calls for the need of new measures for describing the occurrence frequency
401 of extremes, including the clustering of extremes, for serially dependent
402 processes. Waiting time distributions are one promising measure of the reoccurrence
403 properties of extremes. We estimated the exponential distribution and the empirical
404 waiting time distribution for the grid point closest to London (Fig. 8; the results
405 are insensitive to the exact location). The exponential distribution describes the
406 waiting times of a memory-less Poisson process. As can be seen in Fig. 8 the
407 empirical waiting time has a much fatter tail of waiting times than one would expect
408 from a memory-less Poisson process. This is the imprint from the clustering which
409 means that for long periods no extremes occur but when they occur they occur in
410 bunches. The mean waiting time of the Exponential distribution is 14 days, while
411 the empirically estimated mean waiting time is 33 days. This indicates that traditional
412 extreme value statistics can be misleading if it does not take into account the
413 dependence structure of the underlying process. The estimation of return periods of
414 extremes becomes even more complicated when extremes tend to cluster. Then the
415 return period becomes less meaningful. In principle then one would need two measures:
416 the return period of clusters and the return period of extremes in a cluster.
417 Of course, also outside of clusters extremes can occur. Some promising statistical
418 approaches on clustered extremes are described in Fawcett and Walshaw (2006,
419 2007a, 2007b) and the relationship between long-range dependence and extremes
420 is an active topic of current research.

421 While this study has mainly focused on wind speed extremes there are also other
422 atmospheric circulation related extremes like heat waves and droughts which are
423 associated with blocking. The principal difference between both kinds of extremes
424 is that the first are more 'fast' extremes which last a day or two while the latter
425 are more 'persistent' extremes which can last for weeks or longer. Examples are
426 droughts and heat waves. The jet stream regimes are closely linked to blocking
427 (Franzke et al. 2011) and thus will affect the 'persistent' extremes. For instance,
428 the northern jet regime can last up to 3 weeks (Franzke et al. 2011). While most
429 extreme value statistics is well suited to describe 'fast' extremes the statistical model
430 of the 'persistent' extremes is less well developed. At a conceptual level the 'fast'
431 extremes have highly non-Gaussian distributed increments while the 'persistent'
432 extremes can have nearly Gaussian distributed increments. It is likely that the
433 increments of the 'persistent' extremes are very small due to the quasi-stationary
434 character of the phenomenon. An interesting approach to model natural 'persistent'
435 extremes are so-called bursts (Barabasi 2005, Lowen and Teich 2005).

436 In Franzke et al. (2011) evidence has been provided for large interannual vari-

437 ability of the circulation regimes. Because of the potential that global warming
438 might affect the regimes by e.g. changing their frequency of occurrence there is an
439 urgent need for advanced statistical and mathematical tools to detect and attribute
440 circulation changes and changes in extreme events. The approaches put forward by
441 Horenko (2008, 2010) and O’Kane et al. (2012) are promising for this purpose.
442 Possible processes causing the observed interannual variability are amongst oth-
443 ers North Atlantic ocean variability (e.g. Atlantic Multidecadal Oscillation and
444 the Meridional Overturning Circulation), Arctic sea ice decline, stratospheric cir-
445 culation variability, variations in solar forcing or greenhouse gas emissions. More
446 research is needed to disentangle these processes in a systematic way.

447 I would like to thank Chris Ferro and one anonymous reviewer for their helpful comments
448 on an earlier version of this manuscript. This study is part of the British Antarctic Survey
449 Polar Science for Planet Earth Programme. It was funded by The Natural Environment
450 Research Council. The European Centre for Medium Range Forecasts is gratefully ac-
451 knowledged for providing the ERA-40 reanalysis data.

References

452

- 453 Barabasi, A.-L.: The origin of bursts and heavy tails in human dynamics. *Nature*, 435,
454 207-211, 2005.
- 455 Barbosa, S. M.: Testing for deterministic trends in global sea surface temperature. *J.*
456 *Climate*, 24, 2516-2522, 2011.
- 457 Barnston, A. G. and R. E. Livezey: Classification, seasonality and persistence of low-
458 frequency atmospheric circulation patterns. *Mon. Wea. Rev.*, 115, 1083-1126, 1987.
- 459 Beirlant, J., Y. Goegebeur, J. Segers and J. Teugels, *Statistics of extremes: Theory and*
460 *applications*. Wiley, 2004.
- 461 Beran, J., *Statistics for Long-Memory Processes*. Chapman & Hall, 1994.
- 462 Berman, S. M.: Limit theorems for the maximum term in stationary sequences. *Annals*
463 *Mat. Stats.*, 35, 502-516, 1964.
- 464 Blackburn, M., J. Methven and N. Roberts: Large-scale context for the UK floods in
465 summer 2007. *Weather*, 63, 280-288, 2008.
- 466 Bunde, A., J. F. Eichner, J. W. Kantelhardt and S. Havlin: Long-term memory: a natural
467 mechanism for the clustering of extreme records and anomalous residual times in climate
468 records. *Phys. Rev. Letts.*, 94, 048701, 2005.
- 469 Cassou, C.: Intraseasonal interaction between the Madden-Julian Oscillation and the
470 North Atlantic Oscillation. *Nature*, 455, 2008. doi: 10.1038/nature07286
- 471 Cattiaux, J., R. Vautard, C. Cassou, P. Yiou, V. Masson-Delmotte and F. Codron: Winter
472 2010 in Europe: A cold extreme in a warming climate. *Geophys. Res. Lett.*, 37, L20704,
473 2010. doi: 10.1029/2010GL044613
- 474 Cheng, X., and J. M. Wallace: Multiple Flow Equilibria in the Atmosphere Wintertime
475 500 hPa Height Field: Spatial Patterns. *J. Atmos. Sci.*, 50, 2674-2696, 1993.
- 476 Coles, S.: *An Introduction to Statistical Modelling of Extreme Values*. Springer, London,
477 208p, 2001.
- 478 Defant, A.: Oscillations of the atmospheric circulation over the North Atlantic ocean in
479 the 25-year period 1881-1905. *Mon. Wea. Rev.*, 387-393, 1924.
- 480 Fawcett, L. and D. Walshaw: Markov Chain models for extreme wind speeds. *Environ-*
481 *metrics*, 17, 795-809, 2006. doi: 10.1002/env.794
- 482 Fawcett, L. and D. Walshaw: Improved estimation for temporally clustered extremes.
483 *Environmetrics*, 18, 173-188, 2007a. doi: 10.1002/env.810
- 484 Fawcett, L. and D. Walshaw: Bayesian inference for clustered extremes. *Extremes*, 2007b.
485 doi: 10.1007/10687-007-0054-y
- 486 Franzke, C., D. Crommelin, A. Fischer and A. J. Majda: A Hidden Markov Model Perspec-
487 tive on Regimes and Metastability in Atmospheric Flows. *J. Climate*, 21, 1740-1757,
488 2008.
- 489 Franzke, C., I. Horenko, A. J. Majda and R. Klein: Systematic Metastable Atmospheric
490 Regime Identification in an AGCM. *J. Atmos. Sci.*, 66, 1997-2012, 2009.
- 491 Franzke, C.: Long-range dependence and climate noise characteristics of Antarctic tem-
492 perature data. *J. Climate*, 23, 2010, doi: 10.1175/2010JCLI3654.1.
- 493 Franzke, C., T. Graves, N. W. Watkins, R. B. Gramacy and C. Hughes, Robustness of
494 estimators of long-range dependency and self-similarity under non-Gaussianity. *Phil.*
495 *Trans. R. Soc. A*, 370, 1250-1267, 2012.
- 496 Franzke, C. and T. Woollings, On the persistence and predictability properties of North
497 Atlantic climate variability. *J. Clim.*, 24, 466-472, 2011.
- 498 Franzke, C., T. Woollings and O. Martius, Persistent circulation regimes and preferred
499 regime transitions in the North Atlantic. *J. Atmos. Sci.*, 68, 2809-2825, 2011.
- 500 Franzke, C.: Nonlinear trends, long-range dependence and climate noise properties of
501 surface air temperature. *J. Climate*, 25, 4172-4183, 2012a.

- 502 Franzke, C.: Predictability of extreme events in a nonlinear stochastic-dynamical model.
503 Phys. Rev. E, 85, 2012b. doi: 10.1103/PhysRevE.85.031134
- 504 Franzke, C.: Significant reduction of cold temperature extremes in the Antarctic Peninsula
505 at Faraday/Vernadsky. Int. J. Clim., 2012c, doi: 10.1002/joc.3490
- 506 Garrett, C. and P. Müller: Supplement to “Extreme events”. Bull. Amer. Meteor. Soc.,
507 89, 1733, 2008. doi: 10.1175/2008BAMS2566.2
- 508 Geweke, J. and S. Porter-Hudak: The estimation and application of long memory time
509 series models. J. Time Ser. Anal., 4, 221-237, 1983.
- 510 Ghil, M., et al.: Extreme Events: Dynamics, Statistics and Prediction. Nonlin. Processes
511 Geophys., 18, 295-350, 2011. doi:10.5194/npg-18-295-2011
- 512 Hamidieh, K, S. Stoev and G. Michailidis: On the estimation of the extremal index based
513 on scaling and resampling. J. Comp. Graphical. Stat., 18, 731-755, 2009.
- 514 Holzer, M.: Asymmetric geopotential height fluctuations from symmetric winds. J. Atmos.
515 Sci., 53, 1361-1379, 1996.
- 516 Horenko, I.: Finite element approach to clustering of multidimensional time series. SIAM
517 J. Sci. Comp., 32, 62-83, 2008.
- 518 Horenko, I.: On the identification of nonstationary factor models and their application to
519 atmospheric data analysis. J. Atmos. Sci., 67, 1559-1574, 2010.
- 520 Hurvich, C. M. and R. S. Deo: Plug-in selection of the number of frequencies in regression
521 estimates of the memory parameter of a long-memory time series. J. Time Ser. Anal.,
522 20, 331-341, 1999.
- 523 IPCC 2012: Managing the risks of extreme events and disasters to advance climate change
524 adaptation. A special report of working groups I and II of the International Panel on
525 Climate Change [Field, C. B., V. Barros, T. F. Stocker, D. Qin, D. J. Dokken, K. L.
526 Ebi, M. D. Mastrandrea, K. J. Mach, G.-K. Plattner, S. K. Allen, M. Tignor and M.
527 P. Midgley (eds.)]. Cambridge University Press, Cambridge, UK, and New York, NY,
528 USA, 582 pp., 2012.
- 529 Klemes, V: The Hurst phenomenon: A puzzle? Water Resource Res., 10, 675-688, 1974.
- 530 Kimoto, K. and M. Ghil: Multiple Flow Regimes in the Northern Hemisphere Winter. Part
531 II: Sectorial Regimes and Preferred Transitions. J. Atmos. Sci., 50, 2645-2673, 1993.
- 532 Koscielny-Bunde, E., A. Bunde, S. Havlin, H. E. Roman, Y. Goldreich and H.-J. Schellnhu-
533 ber: Indication of a universal persistence law governing atmospheric variability. Phy.
534 Rev. Let., 81, 729-732, 1998.
- 535 Leadbetter, M. R. and H. Rootzen: Extremal theory for stochastic processes. 16, 431-478,
536 1988.
- 537 Livezey, R. E. and W. Y. Chen: Statistical field significance and its determination by
538 Monte Carlo techniques. Mon. Wea. Rev., 111, 46-59, 1983.
- 539 Lowen, S. B. and M. C. Teich: Fractal-based point processes. Wiley Series in Probability
540 and Statistics. 594pp., 2005.
- 541 Luxford, F. and T. Woollings: A simple kinematic source of skewness in atmospheric flow
542 fields. J. Atmos. Sci., 69, 578-590, 2012.
- 543 Mailier, P., D. Stephenson and C. Ferro, Serial Clustering of Extratropical Storms. Mon.
544 Wea. Rev., 134, 2224-2240, 2006.
- 545 Majda, A. J., C. Franzke, A. Fischer and D. Crommelin: Distinct metastable atmospheric
546 regimes despite nearly Gaussian statistics: A paradigm model. Proc. Natl. Acad. Sci.
547 USA, 103, 8309-8314, 2006.
- 548 Majda, A., C. Franzke and D. Crommelin: Normal forms for reduced stochastic climate
549 models. Proc. Nat. Acad. Sci. USA, 106, doi:10.1073/pnas.0900173106, 2009.

- 550 Malmquist, D. L. (ed): European windstorms and the North Atlantic Oscillation: Im-
551 pacts, Characteristics and Predictability. RPI Series No. 2, Risk Prediction Ini-
552 tiative/Bermuda Biological Station for Research, Hamilton, Bermuda, 1999. 21pp.
553 <http://www.bios.edu/rpi/public/pubs/pre2000/euwindsum/eurowindsum.html#fig8a>
- 554 O’Kane, T. J., J. S. Risbey, C. Franzke, I. Horenko and D. P. Monselesan: Changes in
555 the meta-stability of the mid-latitude Southern Hemisphere circulation and the utility
556 of non-stationary cluster analysis and split flow indices as diagnostic tools. *J. Atmos.*
557 *Sci.*, accepted, 2012.
- 558 Press release by Munich Re, 2011: [www.munichre.com/en/media_relations/press_releases/2011/
559 2011.07.12_press_release.aspx](http://www.munichre.com/en/media_relations/press_releases/2011/2011.07.12_press_release.aspx)
- 560 Nakamura, H. and J. M. Wallace: Skewness of low-frequency fluctuations in the tropo-
561 spheric circulation during the Northern Hemisphere winter. *J. Atmos. Sci.*, 48, 1441-
562 1448, 1991.
- 563 Raible, C. C., On the relation between extremes of midlatitude cyclones and the
564 atmospheric circulation using ERA40. *Geophys. Res. Lett.*, 34, L07703, 2007.
565 doi:10.1029/2006/GL029084
- 566 Rahmstorf, S. and D. Coumou: Increase of extreme events in a warming world. *Proc. Nat.*
567 *Acad. USA*, 108, 17905-17909, 2011.
- 568 Rennert, K. J. and J. M. Wallace: Cross-Frequency Coupling, Skewness, and Blocking in
569 the Northern Hemisphere Winter Circulation. *J. Climate*, 22, 5650-5666, 2009.
- 570 Sardeshmukh, P. D. and P. Sura: Reconciling non-Gaussian climate statistics with linear
571 dynamics. *J. Climate*, 22, 1193-1207, 2009. doi 10.1175/2008JCLI2358.1
- 572 Smyth, P., K. Ide and M. Ghil: Multiple regimes in Northern Hemisphere height fields via
573 mixture model clustering. *J. Atmos. Sci.*, 56, 3704-3723, 1999.
- 574 Sura, P.: A general perspective of extreme events in weather and climate. *Atmos. Res.*,
575 101, 1-21, 2011.
- 576 Thompson, D. W. and J. M. Wallace: Regional climate impacts of the Northern Hemi-
577 sphere Annular Mode. *Science*, 293, 85-89, 2001.
- 578 Trenberth, K.E., P.D. Jones, P. Ambenje, R. Bojariu, D. Easterling, A. Klein Tank, D.
579 Parker, F. Rahimzadeh, J.A. Renwick, M. Rusticucci, B. Soden and P. Zhai, 2007: Ob-
580 servations: Surface and Atmospheric Climate Change. In: *Climate Change 2007: The*
581 *Physical Science Basis. Contribution of Working Group I to the Fourth Assessment*
582 *Report of the Intergovernmental Panel on Climate Change* [Solomon, S., D. Qin, M.
583 Manning, Z. Chen, M. Marquis, K.B. Averyt, M. Tignor and H.L. Miller (eds.)]. Cam-
584 bridge University Press, Cambridge, United Kingdom and New York, NY, USA.
- 585 Uppala, S. M., et al., The ERA-40 Re-Analysis. *Quart. J. Roy. Meteor. Soc.*, 131, 2961-
586 3012, 2005.
- 587 Vyushin, D. I., P. J. Kushner and J. Mayer: On the origins of temporal power-law be-
588 havior in the global atmospheric circulation. *Geophys. Res. Letts.*, 36, L14706, 2009.
589 doi:10.1029/2009GL038771
- 590 Walker, G. T. and E. W. Bliss: *World Weather V. Memoirs Roy. Meteorol. Soc.*, 36, 53-84,
591 1932.
- 592 White, G. H.: Skewness, kurtosis and extreme values of northern hemisphere geopotential
593 heights. *Mon. Wea. Rev.*, 108, 146-1455, 1980.
- 594 Woollings, T., A. Hannachi and B. Hoskins: Variability of the North Atlantic eddy-driven
595 jet stream. *Quart. J. Roy. Meteor. Soc.*, 136, 856-868, 2010.
- 596 Yiou, P. and M. Nogaj, Extreme climatic events and weather regimes over the
597 North Atlantic: When and where? *Geophys. Res. Lett.*, 31, L07202, 2004.
598 doi:10.1029/2003GL019119

- 599 Yiou, P., K. Goubanova, Z. X. Li and M. Nogaj: Weather regime dependence of extreme
600 value statistics for summer temperature and precipitation. *Nonlin. Processes Geophys.*,
601 15, 365-378, 2008.
- 602 Yin, J. H. and G. W. Branstator, Geographical variations of the influence of low-frequency
603 variability on lower-tropospheric extreme westerly wind events. *J. Climate*, 21, 4779-
604 4798, 2008.

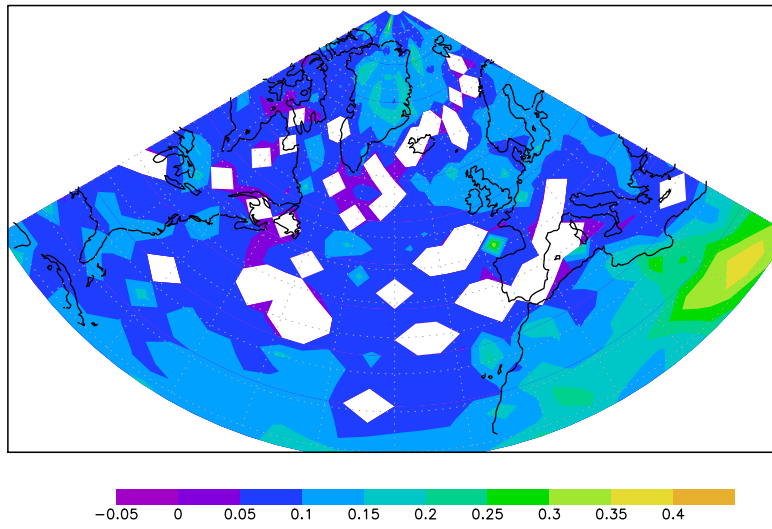


Figure 1. Long-range dependence parameter d of unfiltered surface wind speeds. Only values significant at the 5% level are displayed. Online version in color.

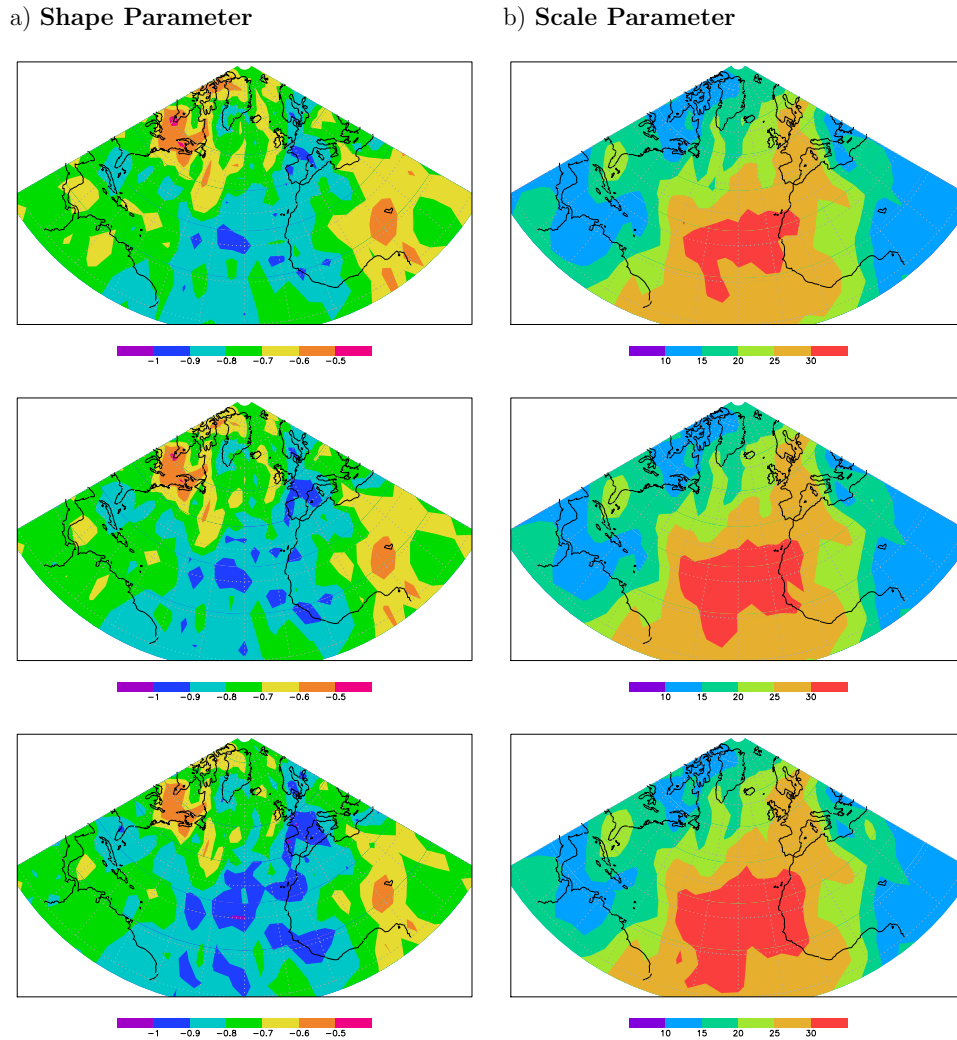


Figure 2. Shape and scale parameter of Generalised Pareto Distribution of unfiltered surface wind speeds for three different thresholds (Upper row: 88th percentile, middle row: 90th percentile and lower row: 92th percentile). Online version in color.

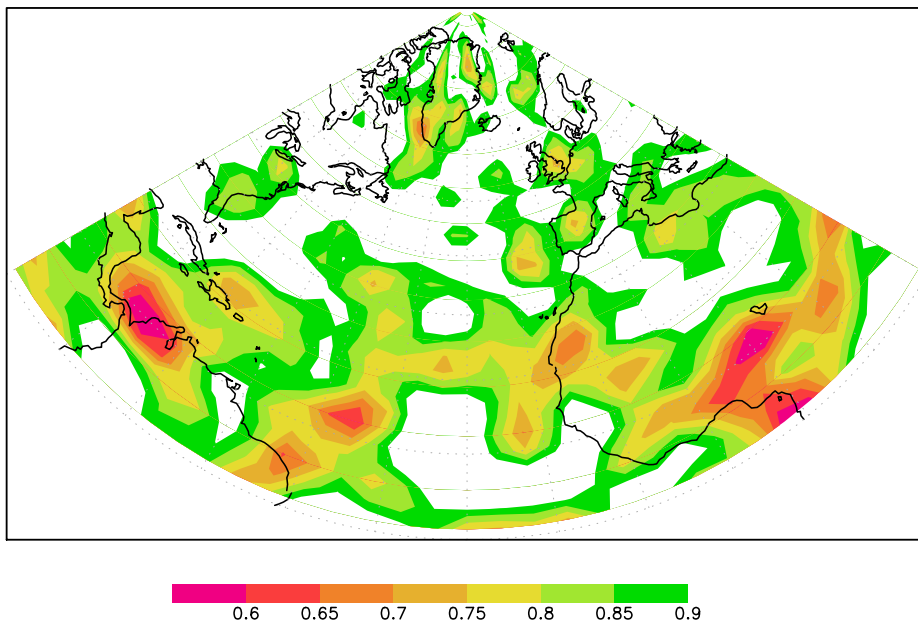
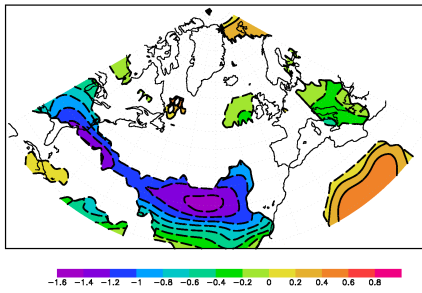
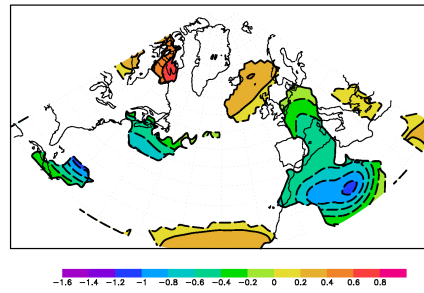


Figure 3. Extremal index of unfiltered surface wind speeds. Displayed are only values which are significant at the 5% level. Online version in color.

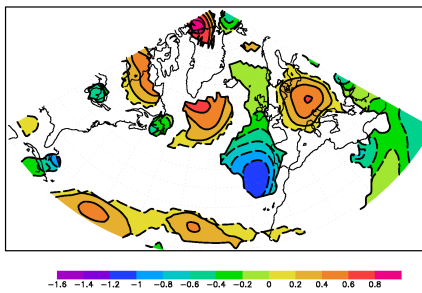
a) Southern Jet



b) Northern Jet



c) Central Jet



d) Climatology

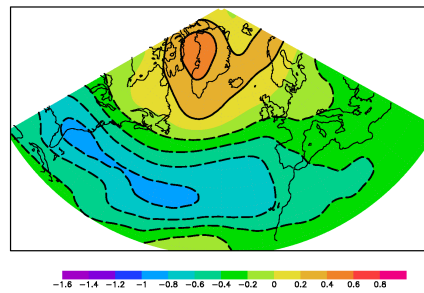
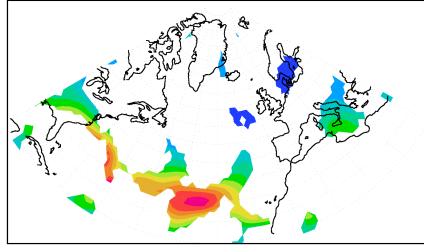
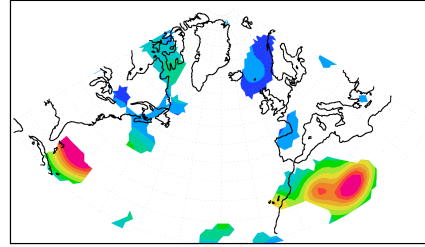


Figure 4. 500 hPa geopotential height skewness. Displayed are only values which are significant at the 5% level. Online version in color.

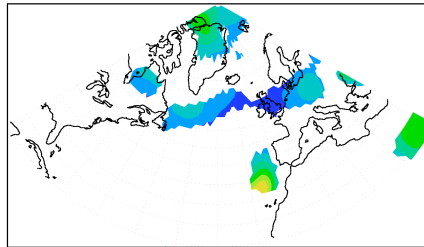
a) Southern Jet



b) Northern Jet



c) Central Jet



d) Climatology

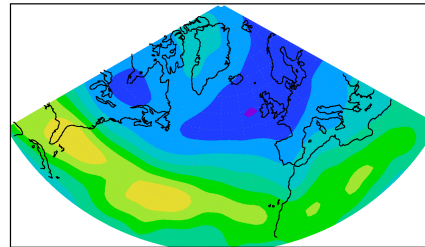
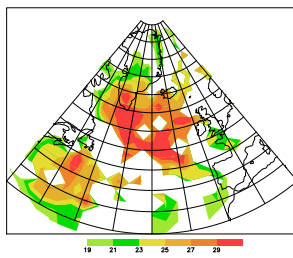
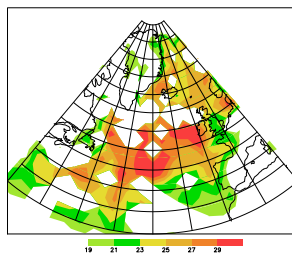


Figure 5. 500 hPa geopotential height kurtosis. Displayed are only values which are significant at the 5% level. Online version in color.

a) Southern Jet



b) Northern Jet



c) Central Jet

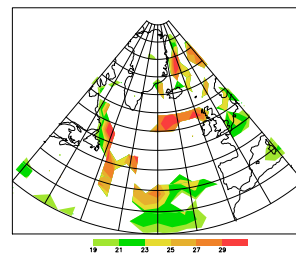


Figure 6. 99.9th percentile of unfiltered surface wind speeds. Displayed are only values which are significant at the 5% level. Online version in color.

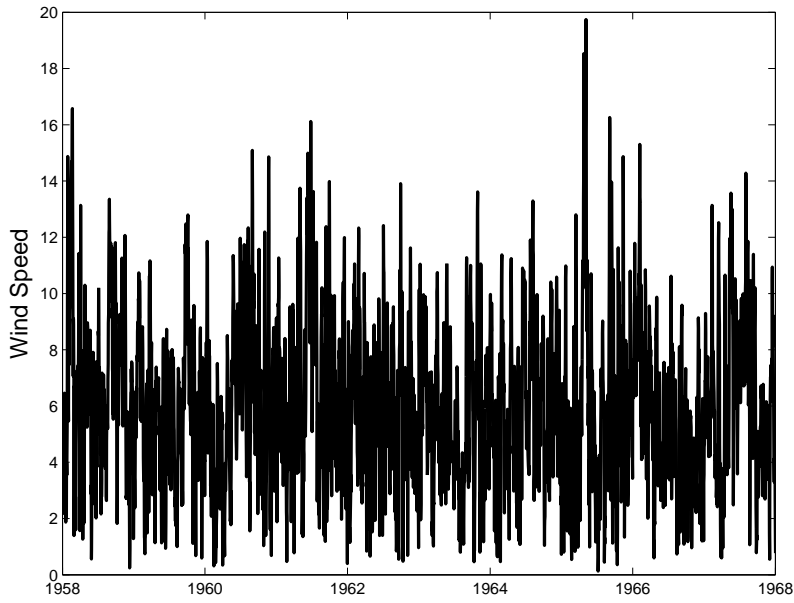


Figure 7. Wind speed time series at a grid point located close to London for the period 1958 through 1968.

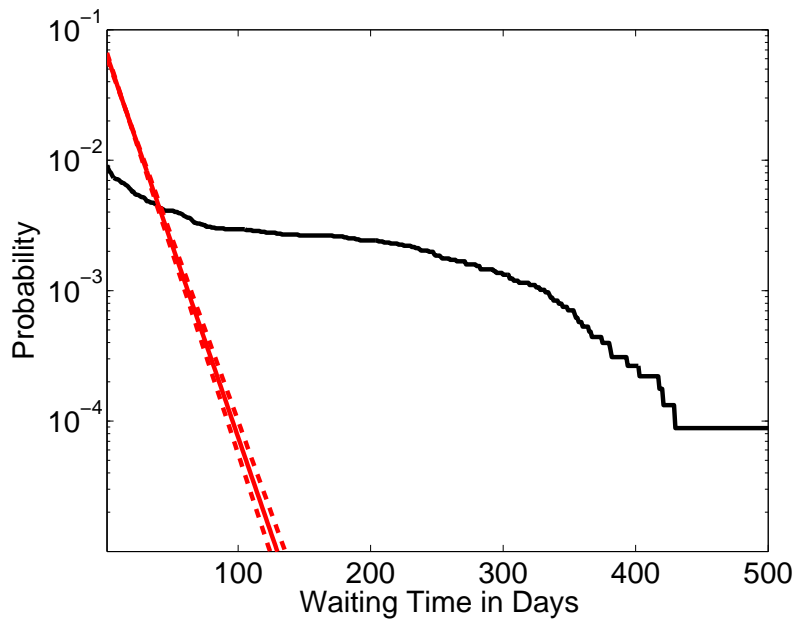


Figure 8. The cumulative waiting time distribution between consecutive 99th percentile threshold exceedances at a grid point located close to London (solid line). Plotted is the probability to exceed the waiting time in days (as given on the x-axis). The crosses denote the corresponding exponential distribution and the dashed lines indicate the 5th and 95th error bounds of the exponential distribution. Online version in color.